Spring 2023

Determining Deuterium Polarization via Nuclear Magnetic Resonance

Nicholas Muche
University of New Hampshire, Durham

Determining Deuterium Polarization via Nuclear Magnetic Resonance

Nicholas Muche
Advisor: Dr. Karl Slifer

A Thesis Presented for the Degree of
Bachelors of Science

Department of Physics and Astronomy
Durham, New Hampshire
May 2023

Contents

Abstract

Dynamic Nuclear Polarization (DNP) is a method by which the spins of electrons are specifically targeted by microwaves at resonance frequency in order to induce spin flips. Occasionally, the electron spins couple with nuclear spins and nuclear spin flips are induced. The relaxation time of the electron is significantly lower than that of the nuclei, which allows for large polarization. The main goal of the Slifer Lab is to utilize specifically prepared crystalline structures in order to separate the convoluted energy transitions ("Batman Peak") in the deuterium's nuclear magnetic resonance (NMR) signal, which would allow for tensor enhancement of deuterium. The goal of this project was to determine the polarizations of deuterium under different conditions from previously taken experimental data and to determine a calibration constant that scales the area under an NMR curve to the polarization. Also, by determining the polarization of deuterium by separate methods, the calibration constant and an independent ratio method, the consistency of the data is checked. The ratio method produced a polarization (0.23287671) that was almost double ($1.73\times$) that of the error method calibration (0.13569978). The ratio method is similar to that of a trusted, independent line-shape method, which indicates an error in the determination of the calibration constant. The source of these issues will be explored further at the end of this paper.

1 Introduction

The field of Nuclear Physics concerns itself with the smallest elements of matter. Of specific interest are the forces and fundamental properties that govern the interactions on the atomic and subatomic scale. The weak and strong nuclear force independently control nuclear stability and have been known since their respective discoveries in the early 1900s. The strong nuclear force having been discovered by Hideki Yukawa [1] and the weak force being discovered by Enrico Fermi [2]. However, these forces do not tell the whole story, as there are intrinsic properties that nuclei and their constituents have that are essential. Examples of such values are spin, angular momentum, magnetic moment, charge, mass/energy among others and they can interact with each other in dynamic ways. For example, there is a potential for spins of nearby particles to couple, or for electromagnetic repulsion/attraction. On

the subatomic scale, quarks are interacting through the exchange of gluons and this interaction is responsible for the formation of protons, neutrons, and therefore the universe as we see it. Quarks have been experimentally determined to be spin-1/2 particles, identical to the proton, and it was originally thought that the proton spin was some linear combination of the constituent spins. As protons are comprised of 2 up quarks and 1 down, it would be logical to assume the different quark flavors are spinning in opposite directions and the resultant sum is that of the un-cancelled up quark. In the 1980's, though, physicists were able to determine that only 25% of the proton spin is due to the quarks (known as "The Spin Crisis") [3]. This leaves the main constituent for the remaining spin as the gluon, which has been shown to be a spin-1 particle. High energy proton collisions are mediated by gluons, so comparing collisions between spin-polarized protons and unpolarized protons should show how much gluon spin effects proton spin (i.e. a 0% difference would indicate gluon spin has no effect on proton spin) [4]. The difference between these data sets is not 0 and so the gluon has an obvious spin contribution. Furthermore, the quarks carry angular momentum (quantum mechanically represented by quantum numbers l and m_l) which is extrinsic. Extrinsic momentum is known to influence intrinsic momentum (spin) in phenomena such as Russel-Sanders coupling, and so it is not a stretch to assume that the extrinsic angular momentum of quarks also influences proton spins. Obviously, these complex Quantum Chromodyanamic (QCD) effects have major implications, such as increasing the understanding of confinement (why quarks and gluons are always found confined in protons and neutrons).

The understanding of the deuteron is lacking. In order to learn about how the overall properties of deuterium are elicited there must be more exploration into its tensor structure. Specifically, by experimental determination of the tensor structure function (b_1), information can be extracted about how the deuterium nucleus ground state deviates from being a composite of nucleons only. The tensor structure also has a connection to the spin-1 angular momentum sum rule (Close-Kumano Rule) [5]. In order to obtain good measurements of the tensor structure, high target and beam polarizations are required for collision experiments. In order to do this, the Slifer Lab has theorized that crystalline targets will increase the peak distance between the spin transitions and therefore maximize tensor enhancement (P_{zz}) which

follows 1 [5].

$$P_{zz} = \frac{(N_+ + N_-) - 2N_0}{N_+ + N_0 + N_-} \tag{1}$$

Where $N_\pm$ refers to the number of particles in the $\pm$ 1 spin state and N_0 refers to those in the 0 state. The equation is normalized by the total amount of particles. The tensor polarization runs from -200% to +100%. In this paper, however, only vector polarization (P_z) is explored. This has the familiar 0-100% distribution, but current polarization efforts have only reached 20-40%; which, is what the crystalline target preparation used in the Slifer Lab tries to address. Vector polarization is only defined by transitions to the +1 or -1 states and is therefore distinct from tensor polarization, which includes particles in the 0 state.

The proton is spin-1/2 and the deuteron is spin-1 and they have distinct NMR peaks for these spin state transitions. The proton has a single peak while the deuteron has 2 due to the extra possible transition. Interestingly, these deuterium NMR peaks are convoluted and the peak distance is not maximized. This means that, as one spin transition is driven, transitions from the other state are also induced due to this mixing. This is what causes such a drastic difference in polarizations between protons and deuterons. If there were a method for decoupling these transitions one could expect significantly higher polarizations of deuterium while also providing essential data for tensor enhancement of deuterium.

These goals of the Slifer Lab require precise measurement of the deuterium NMR signal, while keeping control of variables such as temperature, pressure, field strength, etc. at constant values. The goal of this project is to take data from a previous experiment and determine the polarization of deuterium in 2 separate ways. (1) By determining a calibration constant (C) that can be used to find any deuterium polarization at a given temperature and field strength by multiplying by the area under the enhanced NMR curve and (2) By finding a ratio between peak and shoulder height that can be scaled to the polarization. Finding the polarization by two independent methods checks the consistency of the polarization data and experimental methods. The ratio method produced a polarization (0.23287671) that was almost double (≈ 1.73 $\times$) that of the calibration constant (0.13569978). The ratio method is similar to that of a trusted, independent line-shape method, which indicates an error in the determination of the calibration constant. The source of these issues is heavily dependent on the background subtraction and fitting method used

on the thermal polarization signal. As will be seen below, C is determined exclusively by the experimental parameters T, B, and by the area under the TE curve.

1.1 DNP

Target materials can first be polarized through simple thermal means. This is done by placing the sample in a low temperature and high magnetic field, which results in relatively low polarization percents and follows the form of 2 for spin 1/2 (such as a proton) and 3 for spin 1 (such as deuterium).

$$P_{1/2}^{TE} = tanh(\frac{\mu_p B}{2K_b T}) \tag{2}$$

$$P_{1}^{TE} = \frac{4tanh(\frac{\mu_D B}{2K_b T})}{3 + tanh^2(\frac{\mu_D B}{2K_b T})} \tag{3}$$

Plugging the experimental temperature and field parameters of 1.36K and 5T, along with the known values of μ_p, μ_D, and Boltzmann's constant into these equations gives the thermal vector polarization of the sample. The values obtained are 0.00067250±0.00005082. and 0.00076794±0.00020328, respectively. This is far too low for experimental use, and so DNP is utilized to enhance nuclear polarizations. However, the thermal polarization nuclear magnetic resonance is physically significant, as will be seen in the subsequent sections of this paper.

Dynamic Nuclear Polarization is a process by which nuclear spins can be directly manipulated to have a specific spin orientation. The technique requires either chemical doping or irradiation of the target material to introduce paramagnetic centers. The Solid Effect describes the internal physics of the nuclear spin flipping. It states that the dipole interaction between the free electrons and nuclei leads to hyperfine splitting and coupling of the spins. For spin-1/2 systems, two-level energy spacing is determined by the particle's gyromagnetic ratio (γ), which is directly related to the applied B-field by 4.

$$B = 2\pi\nu\gamma \tag{4}$$

When microwaves are applied near the electron spin resonance (ν_e), transitions are induced, and due to the spin-spin coupling defined by the Solid Effect, as electron spins are flipped the nuclei spins are also flipped. This

process is effective due to the drastically different relaxation times between the electron and nuclei. The electron relaxation time is on the order of microseconds, while the nuclei are on the order of several minutes. So each electron is able to couple, flip, relax, and repeat before any nuclei are able to relax, which can result in polarizations of 90% for protons and 40% for deuterons.

1.2 Material Preparation

Chemical doping of the sample is done by introducing a stable radical to a liquid, then flash freezing the liquid to ensure homogeneous electron distribution [6]. One method of flash freezing is the drop method, which is done by using a burette to introduce individual droplets of sample liquid into a bath (typically of liquid nitrogen, but any non-interacting, sufficiently cold bath will work), which flash-freezes the droplet into a highly homogeneous, amorphous, sphere [7]. At the University of New Hampshire (UNH), in the Slifer Lab, all targets are prepared through chemical doping methods, as it allows for greater control of sample qualities, such as homogeneity and density.

1.3 NMR

Nuclear Magnetic Resonance is a process in which molecules are placed in a static magnetic field, which aligns them according to their magnetic moment. Then, a smaller, oscillating magnetic field is applied and this causes a perturbation from the original alignment. This movement causes the nuclei to produce electromagnetic waves in radio frequency (RF) which can be tracked with a pickup coil. At UNH, a VME crate-based NMR system developed at Los Alamos National Laboratory (LANL) [8] is used. When a target particle undergoes a spin transition it will either release or absorb a photon, depending on the direction of polarization. These photons have the familiar energy 5.

$$E = hf \tag{5}$$

When the target is surrounded by a coil inductor connected to a LRC (inductance-resistor-capacitance) circuit, the incident photon has the potential to couple with the circuit inductance. This results in a measurable impedance spike at the Larmor frequency of the target material. However, the magnetic field is not perfectly uniform and different molecules in the sample are in slightly different fields, which creates a spectrum of spikes,

creating the NMR signal [6]. The Larmor frequency is dependent only on the gyromagnetic ratio, which follows 7, and the oscillating magnetic field.

$$\gamma = \frac{g_n Q}{2m} \tag{6}$$

Which can be redefined with the Nuclear Magneton as

$$\gamma = \frac{g_n \mu_n}{\hbar} \tag{7}$$

From here, the Larmor frequency can be written according to 8.

$$\omega = \gamma B \tag{8}$$

Where omega is the angular processional frequency of the photon. In other words, with a classical description, ω describes the rate at which the magnetic moment precesses around the external field [9]. Furthermore, because the signal is being obtained through a pickup coil connected to a circuit, the resonant frequency is dependent on the inductance and capacitance of the circuit as well, which goes as 9 [6].

$$f = \frac{1}{2\pi\sqrt{LC}} \tag{9}$$

The observations of this circuit result in figures such as those seen in 1 and 2, where the respective single and double peaks are clearly visible. The area under these curves is directly proportional to the vector spin polarization of the target material, which can be used in conjunction with 3 to create a ratio between area and polarization percent. This ratio allows for quick polarization determination for any NMR area. The deuterium graph shows the convoluted spin transitions that come about due to the quadrupolar interaction, whose Hamiltonian follows 10.

$$H_Q = \frac{1}{2}[\sum_{i,j=1}^{3} V_{ij} Q_{ij}] \tag{10}$$

Where V is the electric field gradient and Q is the nuclear quadruple [10]. Notice, also, the difference in frequency between these two graphs. The Larmour frequency changes drastically between the two nuclei and so the centroids are far apart.

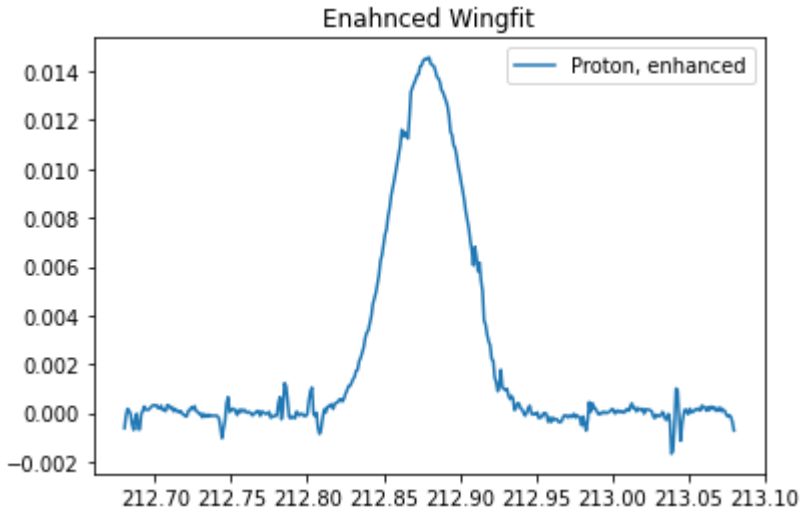

Figure 1: This graph is an example of an enhanced proton polarization NMR signal picked up by the LRC circuit. It has only one peak because transitions in spin states can only be driven between the plus and minus states. The x-axis is MHz and the y-axis is scaled units of voltage (as the signal comes from a pick-up coil in an LRC circuit).

1.4 Zeeman Splitting

In NMR, molecules are placed in a strong static magnetic field, then a smaller, oscillating field is introduced. When nuclei are placed in an external magnetic field, the field couples to the magnetic moments in the atom. The magnetic moment is associated with the orbital and spin angular momentum. [11]. The perturbed nuclei undergo hyperfine splitting of spectral lines (electromagnetic signals i.e. photons) at specific frequency. The slightly different positioning in the field causes different photon energies, which in turn creates the spectrum of signals seen in the NMR. The Zeeman Effect is well defined by the Hamiltonian seen in 11.

$$\hat{H} = -\vec{\mu} * \vec{B} \tag{11}$$

Where μ is the magnetic moment of the molecule in the field and is strongly dependent on the quantum operators $\hat{S}$ and $\hat{L}$, as seen in 12 [11]. In this case, μ is defined for an electron orbiting a proton, as seen in hydrogen and

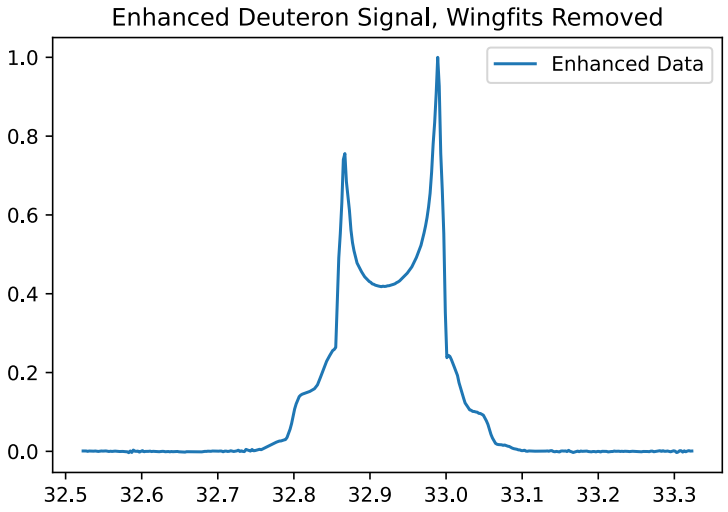

Figure 2: The enhanced data for the sample of deuterated propanediol shows the convoluted transitions (the "Batman Peak"). As deuterium is a spin 1 system, there are three possible states and therefore transitions can be driven in and out of this extra degree of freedom, resulting in a double peak.

analogously in deuterium.

$$\mu = \frac{e}{2m_e}(g_s\hat{S} + g_e\hat{L}) \tag{12}$$

The energy splitting can be written using the landé g-factor and μ as 13

$$\Delta E = g_L \ \mu \ m_j \ \vec{B} \tag{13}$$

Where m_j is the quantum number referring to the projection of the total angular momentum along a specific axis and is defined by a linear combination of the familiar quantum numbers l and s.

At relatively small fields the fine structure correction dominates the Zeeman Effect and so determining the energies is more mathematically difficult, so it's beneficial to utilize strong fields (on the order of several tesla in the context of this paper) to induce splitting in these cases.

The magnetic field exerts a torque on the magnetic moment, forcing it to align or anti-align with the magnetic field lines. As the oscillating field

precesses the magnetic moment of the molecule will precess, which is known as Larmor Precession. The frequency of precession is defined by 8. The frequency here is the frequency of the photons emitted from the energized nuclei and is directly related to their energy [9]. The energy of the photons is defined by their excitation in 13.

2 Methods

The sample used for this experiment was Propanediol-d8 doped with Finland. The methodology of this data analysis project was relatively straight forward. The Slifer lab already had thermal (TE) and vector (enhanced) polarization data for deuterium and hydrogen previously, which I then imported into python for analysis. The first data set analyzed was the thermal and enhanced polarization data for hydrogen. This was done mainly as a reference to explicitly show the complications that arise when a neutron is added to the system. The simple hydrogen data can be seen in 1 and 3. These are not graphs of the raw data. They have had the background removed and functions fit to them. The background was subtracted by taking several subsequent background measurements, averaging them, and removing that average from the data set by simple element subtraction. The fitting method for both hydrogen data sets was done using the curve fit function in the SciPy library on the wings of the signal.

2.1 Enhanced and Thermal Polarization

The fitting of the enhanced deuterium NMR was a more involved process, however. The enhanced data for the deuterium sample was analyzed similarly to the hydrogen sample. All of the deuteron data used for this analysis was taken on 9/14/2020. First, a set of background signals were averaged from 6:09:07 pm to 6:12:59 pm and a single row of enhanced data was taken from 8:44:53 pm. For more accurate results there should be more enhanced data used and averaged in order to assuage the effects potential outliers have on the results. The resultant signal has residual quadratic wings that must be removed, as they are not associated with the physical phenomena being explored. In order to do this, the peak distance in the NMR signal had to be determined, as it has been found quite recently by Michael Mclellan that the entire NMR signal exists between (about) 3 times this distance, and so the

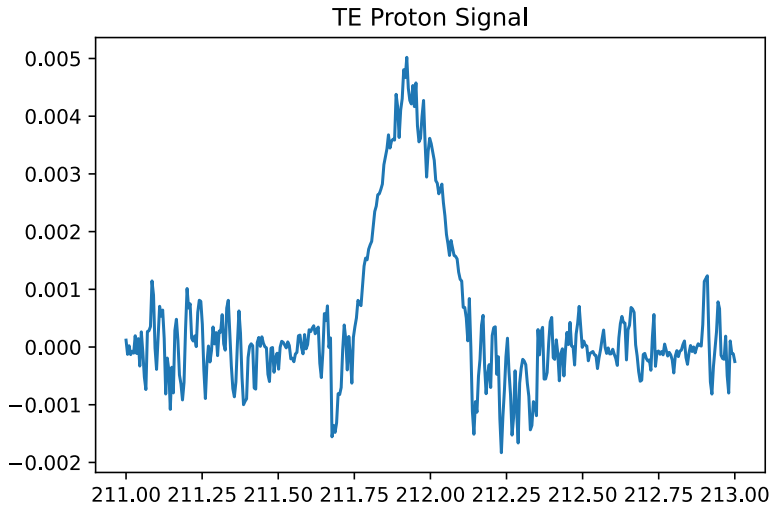

Figure 3: The TE signal for the proton is shown in this figure. It has the same single peak structure, however the amplitude is significantly smaller, as transitions are only driven through thermal means. This means the noise in the circuit is much more noticeable. The data follows the theoretical polarization equation 2. The x-axis is MHz and the y-axis is in scaled units of Volts.

wings were considered to be the portions outside of this range. By appending the data corresponding to these wings to new lists and fitting them with a second order polynomial, fit parameters of the form 14 could be determined. Then, by extrapolating the a_0, a_1, a_2 terms to the entire data set, the residual quadratic was removed.

$$a_0 x^2 + a_1 x + a_2 \tag{14}$$

From here, we get 2, which can be integrated to find the area under the curve. This was done using the trapezoidal integration function ("trapz") in the Numpy python package. Similarly, the TE signal was taken from 6:23:03 pm to 6:28:59 pm and averaged over this interval. The same background was removed from the TE as the enhanced, and a similar method for fitting the wings was applied; with fit parameters b_0, b_1, b_2 following the form of 14. However, the size of the TE signal is a potential issue for the analysis of the NMR because the amplitude of the data is of a small scale, similar to that

of the noise. That is why the TE seen in 4 has visible noise and 2 does not. Both graphs, the TE and enhanced, are graphed over frequency. The central frequencies were considered to be at 32.925 MHz in both cases.

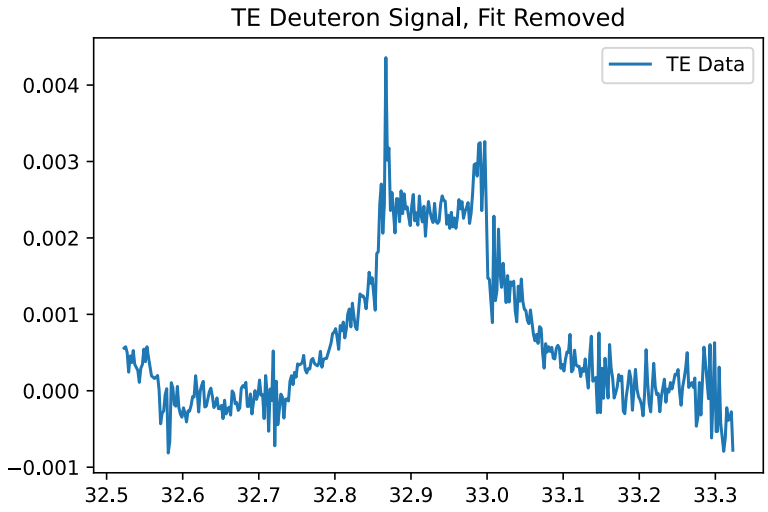

Figure 4: The deuterium TE signal. The centroid is at the same frequency as the enhanced signal, however the scale of the voltage (y-axis) in the pickup coil is significantly smaller, which is directly related to the small polarizations seen from thermal means.

2.2 Graphical Steps

The following series of graphs shows how the enhanced signal was extracted from the raw data. The steps for the TE data were identical, however the enhanced was chosen because the larger magnitude makes the important aspects visible. These are the corresponding graphs for the steps outlined in section 2.1.

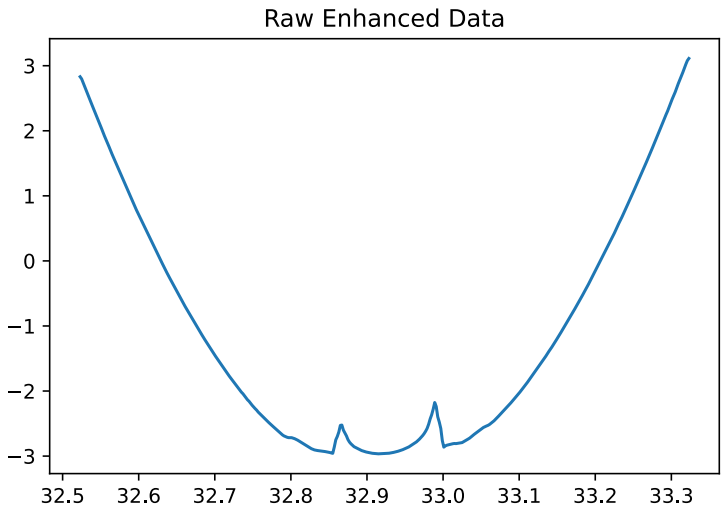

Figure 5: The raw signal shown in this figure is un-edited. It shows a form similar to the baseline, however the enhanced signal is sitting atop the baseline. It is from 9/14/2020 and is a single line of data taken at 8:44:53 pm.

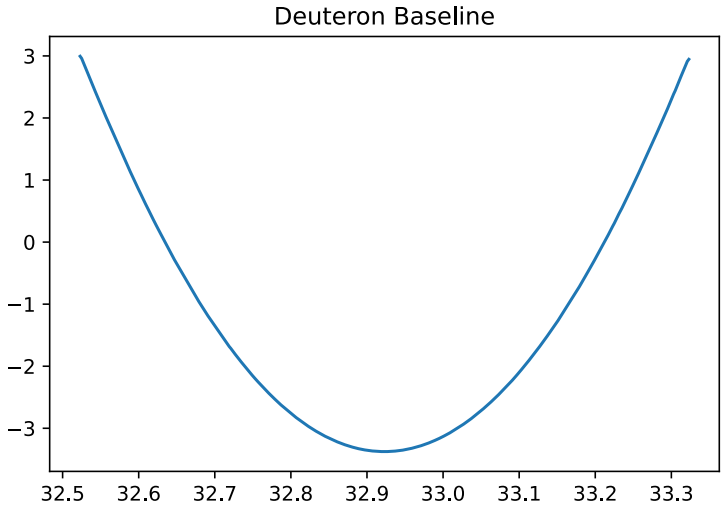

Figure 6: This is the average baseline summed over 6:09:07 pm to 6:12:59 pm on 9/14/2020. It is the signal extracted from the circuit when no target material is present.

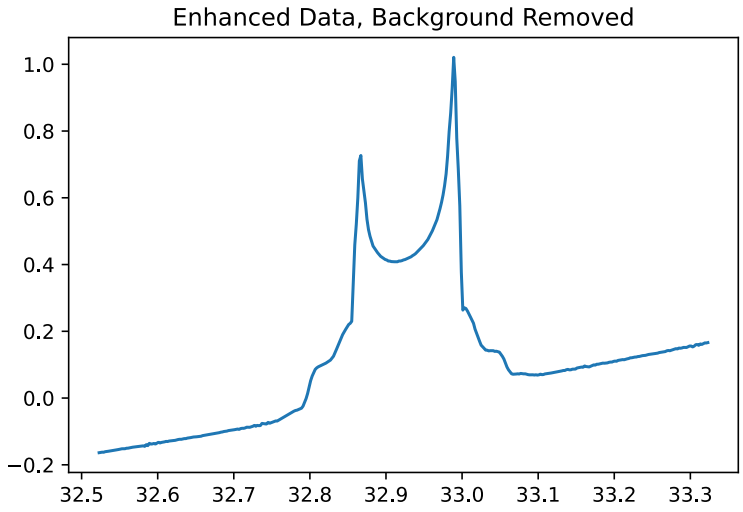

Figure 7: Enhanced data with the baseline removed. As can be clearly seen in the figure, the signal does not go to 0 on the sides, which will add extra area when integrating, so these sections must be removed.

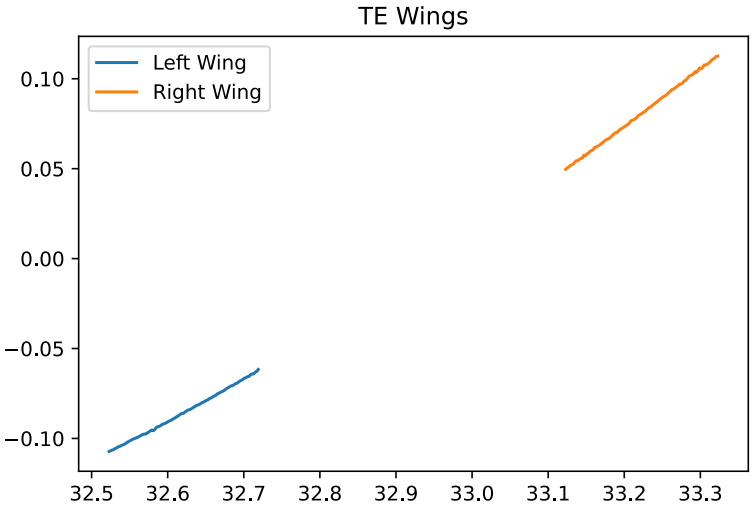

Figure 8: These are the wings seen without the signal in the previous figure. The wings were considered to be the portions of the graph outside 3× the distance between the peaks. This data was fit with a 2nd order polynomial which defined the coefficients used in the subsequent step.

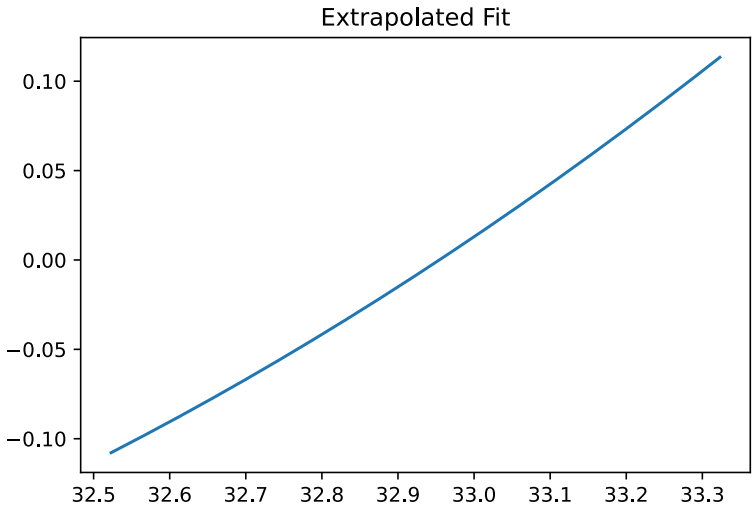

Figure 9: This graph shows the 2nd order fit of the wings. The coefficients from the previous step were used to make a function with the same length as the enhanced data (by inputting the frequency for x in 14). Then, the fit seen in in this graph was subtracted element wise from Figure 7.

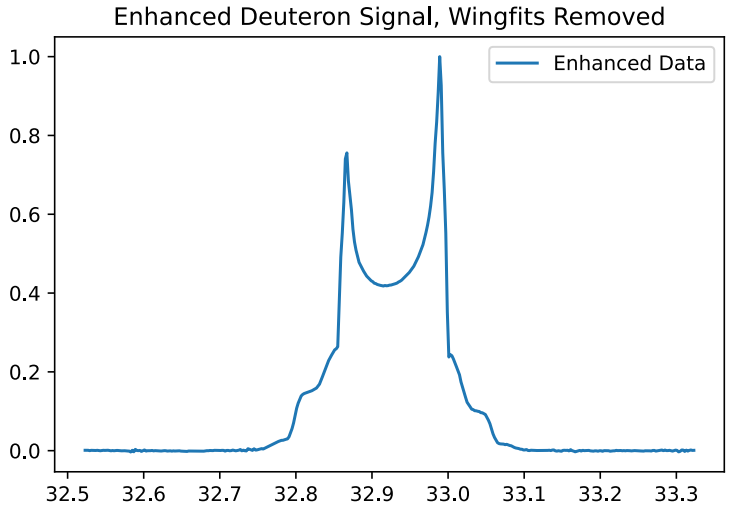

Figure 10: This is the final enhanced graph. Notice how the wings now go to 0 and the non-physical, extra area has mostly been removed. This graph shows the raw data with the baseline and 2nd order wing-fit removed.

2.3 Calibration Constant

The determination of a calibration constant for a set of polarization data is inherently valuable. Using the calibration constant, the area under any NMR curve can be turned into a polarization percent. The calibration constant follows the form of 15 and can be used as in 16 to determine the polarization from the area. It can easily be seen that dividing the theoretical polarization by the area under the curve produces the calibration constant C.

$$C = \frac{P_D}{Area_{TE}} \tag{15}$$

Where P_D is the theoretical polarization determined by 3, which only depends on field strength and temperature.

$$P_z = C * area \tag{16}$$

Plugging in the TE integration value of 0.27026732 and the theoretical P_D value of 0.00076794±0.00020328 into 15 gives a C value of 0.00284141±0.00020328.

2.4 Ratio (R) Method

The ratio method utilizes the ratio between peak and "shoulder" height in order to determine a constant that can be used to determine both vector and tensor polarization. These characteristics of the graph are easiest to see on the enhanced data, as the noise does not interfere greatly with the data. The shoulders occur at about 32.8 MHz for the left and 33.03 MHz for the right. The values are $R_1 = .75, R_2 = .19, L_1 = 1, L_2 = .20$ where R_1 and R_2 are the left peak and shoulder and L_1 and L_2 are the left, respectively. These values can be used to define the overall R constant in 17. Then, 18 and 19 are used find the expected vector and tensor polarizations. Theoretically, this method would match that of the calibration constant method for perfectly fit and aligned data.

$$R = \frac{R_2 - R_1}{L_2 - L_1} \tag{17}$$

$$P_z = \frac{R^2 - 1}{R^2 + 1 + R} \tag{18}$$

$$P_{zz} = 2 - \sqrt{4 - 3P_z^2} \tag{19}$$

Or similarly, the tensor polarization equation can be defined without the vector polarization as 20.

$$P_{zz} = \frac{R^2 - 2R + 1}{R^2 + R + 1} \tag{20}$$

Using 17 the R constant was determined to be 0.70000 when the peak and shoulder values were determined by eye. Then, by 18, the vector polarization was determined to be 0.23287671±0.00020328.

3 Results

At a field strength of 5T and a temperature of 1.36K the expected value for the thermal vector polarization (P_z) of deuterium is 0.00076794±0.00020328 and, dividing by the TE area (0.27026732), gives a calibration constant of 0.00284141±0.00020328 in units of 1 over area, where the actual unit of area is arbitrary as long as it matches the area input into 16. For this specific data set, multiplying any NMR area by C will give the polarization percent of the deuterium sample. So, inputting the area under the enhanced curve (47.75790864) into 16 we find $P_z = 0.1356998 \pm 0.00020328$ (≈13.6%). Doing the similar calculation using the R method we find R = 0.70000 and the magnitude of $P_z = 0.23287671 \pm 0.00020328$ (≈23.3%). The R method does give a negative value for P_z, however simply redefining the ratio in 17 as the reciprocal produces the same polarization, but now positive. The difference between the magnitude of the two methods is 0.09366949, which is nearly a 10% absolute difference in the two methods. Or, the R method produces a polarization ≈1.72× that of the calibration constant method and is therefore showing a 172% relative difference.

4 Error Analysis

Utilizing 21 [12], and a function of the form q(x...z), the uncertainty in the thermal deuterium polarization can be found.

$$\delta q = \sqrt{((\frac{\partial q}{\partial x})\delta x)^2 + ... + ((\frac{\partial q}{\partial z})\delta z)^2} \tag{21}$$

This equation shows the derivative of q taken with respect to each pertinent variable, multiplied by by it's uncertainty, squared, added, and square

rooted. However, the uncertainty in the magnetic moment and Boltzmann constant obtained from NIST are extremely small compared to that of the temperature and are therefore negligible. The magnetic field strength is stable to a about .0001 (about 1000× smaller than the temperature uncertainty) and was also considered negligible. Utilizing the quotient and chain rules to take the derivative of 3, then plugging into 21 with T = 1.36, δT = .12, B = 5.00 T, μ_D = (4.330735094±0.000000011)×10^{-27} and K_B = 1.380649 ×10^{-23} (which NIST expresses as exact) [13] gives a vector polarization uncertainty of 0.00020328. Therefore, the deuterium polarization is 0.00076794±0.00020328. The same method can be used to find the uncertainty in proton polarization, which is 0.00005082 and, therefore, 2 gives 0.00067250±0.00005082.

4.1 Background

The background sample for this set of data is most likely flawed. This is best shown through simple graphical analysis 11. This figure clearly shows that there is a linear relation between the background signal and the TE signal, which is not the appropriate relationship. Removal of the background from the TE should produce an obvious NMR signal, but with this data set a second order polynomial had to be removed before a signal could be seen. Further experimentation should take special care when determining the background signal, as the parameters (field strength and temperature) have a strong effect on the signal. However, as the next section explores, the temperature is probably not the issue.

4.2 Temperature

Figures 12 and 13 show the temperatures over the time frames used for their respective average. The enhanced data is a single line and so the temperature here was obviously constant. The uncertainty in temperature was determined from this figures and as can be seen in the TE figure the temperature spikes around bin 20. Future TE analysis should be careful to remove data with temperatures of this form in order to decrease the uncertainty in results. The temperature uncertainty is simply the difference in minimum and maximum value on these graphs, which is the δT utilized in the error propagation. The uncertainty in temperature is simply the uncertainty of that in the baseline plus the TE, as they were combined through element subtraction [12].

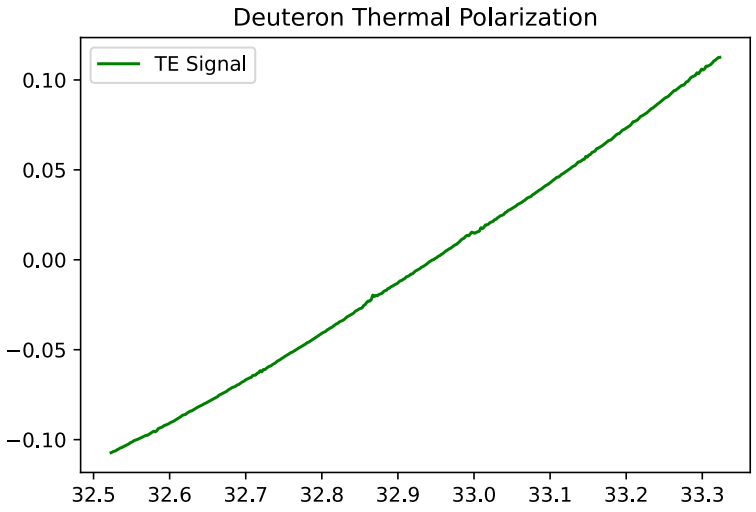

Figure 11: The TE signal after removing the baseline. The TE signal is hard to see, but is sitting atop the line. This indicates a linear relation between the TE and baseline, which is indicating an inappropriate baseline. The y- and x-axis are the familiar scaled volts and frequency.

4.3 Calibration Constant and R method

As previously mentioned, the calibration constant was determined through integration of the TE signal through the trapezoid method. Unfortunately, the method does not have a built in error analysis and so the exact uncertainty is unknown. In order to determine the error in the integration, a function is required to propagate the uncertainty. This would include fitting the NMR signal with a function, integrating by normal definite integration, and propagating the error through it; which, could be done with polynomial interpolation or, because the form of the NMR is well known, a simple Gaussian fit. However, qualitatively, it is well known that for concave down functions the trapezoidal method produces an underestimate of the area. This means the calibration constant is larger than it should be, indicating an even greater discrepancy in methods than this analysis shows. Due to this, and in conjunction with equations 15 and 21, the uncertainty in the calibration constant is the same as that of the P_D. Similarly, the uncertainty in the R method is unknown. Finding the peak values is a simple list compre-

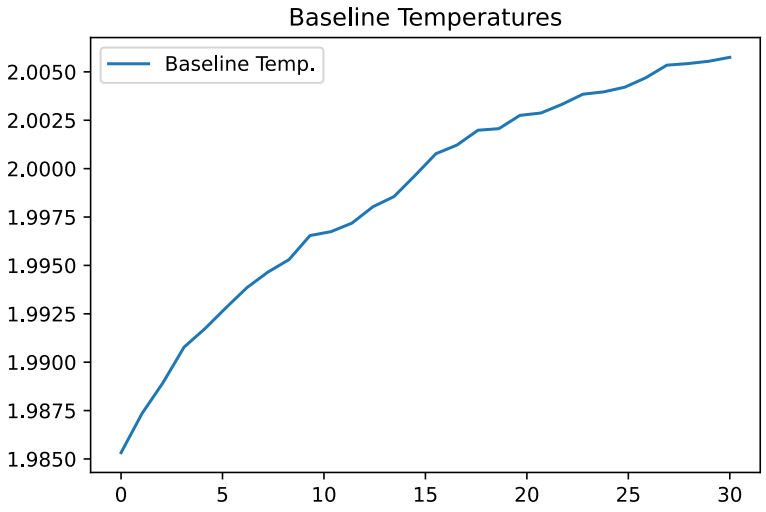

Figure 12: The baseline temperatures graphed over bin number. The y-axis is in kelvin and the amplitude was considered to be 0.03.

hension problem, however finding the shoulder values is much more difficult. For this reason, the height/shoulder difference was fit by eye and therefore has unknown error. However, a previous analysis utilizing a well trusted line-shape method performed by Dr. Nathaly Santiesteban determined the polarization through the R method to be 26.3%. This is in good agreement with the 23.3% determined through this analysis, and so the method used with R here can be considered relatively accurate. The large difference in the 2 methods used in this analysis shows a systematic error in the evaluation of the TE signal. Due to the noise in the circuit being on the same order of magnitude as the TE signal, subtraction of the baseline from the TE introduces inaccuracies which make the wing-fit subtraction difficult. It is most likely that the background subtraction and wing fit are adding structure to the TE signal and by extension increasing the area and decreasing C. In order to address this issue, the nuclear group should take significantly longer TE's and baselines in order to cancel out the fluctuations when the signals are time averaged.

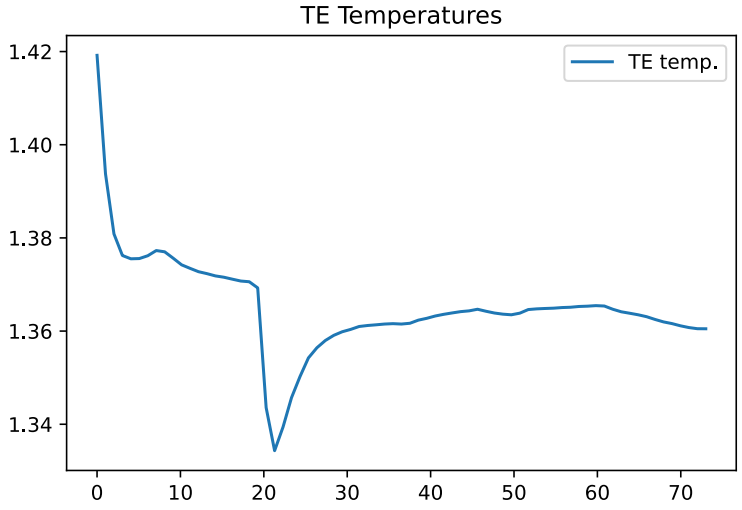

Figure 13: The baseline temperatures graphed over bin number. The y-axis is in kelvin and the amplitude was considered to be 0.09 K.

5 Summary

My work in the Slifer Lab began with watching/assisting Keeyote Slover-Carpenter in the material preparation aspect of his senior thesis. I was able to watch him do an ammonia (NH_3) solidification in the Demerit chemistry lab while also learning about the specific aspects that go into the solidification process. This is where I was first exposed to the drip method, but I was also able to learn about the rapid solidification and cold finger methods. These processes are similar, however the cold finger method utilizes a copper shell inside the cryostate which slows the cooling process and increases the resulting crystalline structure. Also, this is when I started to read the relevant papers written by the nuclear group describing the DNP process.

Once I understood the main background ideas relating to DNP, such as Zeeman Splitting, the Solid Effect and Spin-Spin coupling, I was able to delve into the main part of my project, which was NMR analysis. This began with learning how NMR works in general, with nuclear excitations and eventually going into essential ideas such as Larmor Precession. Then transitioning to the specific characteristics of the proton and deuteron NMR and what physical processes elicit them. The convoluted NMR peak seen in deuterium

being due to mixing of spin transition states, creating the "shoulders" on the signal and how maximizing the peak distance (de-convolution) is one of the goals of the crystalline structures.

Finally, I was given a data set for a polarization experiment with propanediol-d8 doped with finland in order to determine the polarization via the NMR signals. To do this, I had to learn even more about the characteristics of the signals, relevant polarization equations, and, especially, about Python. The majority of the work done in this project was in Python and it started with list comprehension. The thousands of lines of data were importing as a single variable string, so I had to sort them in Python by importing the data as a string, determining delimiters, sorting the strings into appropriate rows, and finally converting all the data to usable floats. Then, once I had data that could be worked with, I was able to graph the respective TE and enhanced NMR's and perform the analysis. I created the code to be as general as possible and, hopefully, it will be useful for further use in the nuclear group for polarization experiments.

6 Acknowledgments

I would like to personally thank Dr. Karl Slifer for advising me on this project and for providing the necessary materials and assistance. I would also like to thank Dr. Elena Long for her assistance with some coding aspects of this project. A special thanks to Keeyote Slover-Carpenter and Anderson Stecklei for peer reviewing this paper and code. And finally, a thank you to the Nuclear Group and the physics department at the University of New Hampshire for their help and guidance, both direct and indirect, along the way.

References

[1] Laurie M. Brown. *Hideki Yukawa and the Meson Theory. Physics Today*, 39:55, 1986.

[2] Enrico Fermi. *An attempt to a rays theory. Nuovo Cimento*, 1:1–20, 1933.

[3] The NNPDF Collaboration. *A first unbiased global determination of polarized PDFs and their uncertainties. Physics Review Letters*, 113, 2014.

[4] Daniel de Florian, et al. . *Evidence for Polarization of Gluons in the Proton. Physics Review Letters*, 113, 2014.

[5] et. al K. Slifer. The deuteron tensor structure function b1. 2019.

[6] K. Slifer, et. al. Solid polarized target system at the university of new hampshire. 2023.

[7] Keeyote Slover-Carpenter. Preparation of solid polarized target material for dynamic nuclear polarization. 2022.

[8] et. al P. McGaughey. A modern q-meter system to measure the polarization of solid polarized targets. *Nuclear Instruments and Methods in Physics Research Section A: Accelerators, Spectrometers, Detectors and Associated Equipment*, 995:165045, 2021.

[9] John S. Rigden. Quantum states and precession: The two discoveries of nmr. *Rev. Mod. Phys.*, 58:433–448, Apr 1986.

[10] et. al F. Tran. Nuclear hyperfine interactions. 2018.

[11] David H. McIntyre. Quantum mechanics. 2012.

[12] J.R. Taylor. Introduction to error analysis. 1982.

[13] The national institute of standards and technology reference on constants, units, and uncertainty, 2023.